Joint Beamforming for RIS Aided Full-Duplex Integrated Sensing and Uplink Communication

Yuan Guo[1], Yang Liu[1*], Qingqing Wu[2], Xin Zeng[3], and Qingjiang Shi[4]
[1]School of Info. and Commun. Eng., Dalian University of Technology, Dalian, China
[2]Department of Electronic Engineering, Shanghai Jiao Tong University, Shanghai, China
[3]College of Electronic and Information Engineering, Tongji University, Shanghai, China
[4]School of Software Eng., Tongji Univ. Shanghai, Shenzhen Research Institute of Big Data, Shenzhen, China
E-mails: yuanguo@mail.dlut.edu.cn, yangliu_613@dlut.edu.cn, qingqingwu@sjtu.edu.cn, zengxin1@tongji.edu.cn, shiqj@tongji.edu.cn

***Abstract*—This paper studies integrated sensing and communication (ISAC) technology in a full-duplex (FD) uplink communication system. As opposed to the half-duplex system, where sensing is conducted in a first-emit-then-listen manner, FD ISAC system emits and listens simultaneously and hence conducts uninterrupted target sensing. Besides, impressed by the recently emerging reconfigurable intelligent surface (RIS) technology, we also employ RIS to improve the self-interference (SI) suppression and signal processing gain. As will be seen, the joint beamforming, RIS configuration and mobile users' power allocation is a difficult optimization problem. To resolve this challenge, via leveraging the cutting-the-edge majorization-minimization (MM) and penalty-dual-decomposition (PDD) methods, we develop an iterative solution that optimizes all variables via using convex optimization techniques. Numerical results demonstrate the effectiveness of our proposed solution and the great benefit of employing RIS in the FD ISAC system.**

***Index Terms*—integrated sensing and communication (ISAC), reconfigurable intelligent surface (RIS), full-duplex (FD).**

I. Introduction

Very recently, the integrated sensing and communication (ISAC) system has been cast with great attentions from both industry and academia [1] − [2]. The ISAC system aims at realizing both radar sensing and communication functionalities using one unified hardware set and overlapping spectrums. The ISAC technology is highly meaningful in improving hardware and spectral efficiency and making wireless devices more amiable to diverse internet of things (IoT) applications in future.

At the same time, the recently rising reconfigurable intelligent surface (RIS) [3], which is also widely known as intelligent reflecting surface (IRS) [4], has also been envisioned as a viable solution to enhance the next generation wireless communication system. Via reflecting the electromagnetic waves and wisely adjusting their phase shifts, the RIS entitle the wireless network with a novel *passive* beamforming capability at a low hardware and energy cost [3]−[4]. The potentials and versatility of RIS has been extensively explored recently, e.g., see [3]−[4] and the reference therein.

In light of the recent booming RIS technology, a number of latest works are exploring to employ RIS to enhance the ISAC system's performance [5]−[9]. For instance, the authors in [5] and [6] studied minimizing multi-user interference (MUI) while satisfying the beampattern and the Cramér-Rao bound (CRB) constraints, respectively. The work [7] investigated the radar output signal-to-noise-ratio (SNR) maximization problem under the communication quality of service (QoS) constraint. The paper [8] maximized the weighted sum of the radar SNR and the communication SNR in an RIS-aided ISAC system. The recent literature [9] investigated the transmit power minimization while assuring the cross-correlation pattern design. Note that the existing literature usually considers downlink communications and classical half-duplex (HD) BS.

In this paper, we consider an RIS aided full-duplex (FD) ISAC system, where multiple mobile users operate uplink (UL) communication with the assistance of RIS employed in the vicinity. We aim to maximize the mobile users' throughput while assuring the radar sensing quality is maintained above a reasonable level. The main contributions of this paper are elaborated as follows

- This paper considers an RIS aided FD ISAC system, where the UL communication and mobile users' power allocation is considered, which has rarely been discussed in relevant literature.
- The joint optimization of the active and passive beamforming and power allocation is highly challenging. By virtue of majorization-minimization (MM) [10] and penalty-dual-decomposition (PDD) [11] methods, we propose an alternative optimization solution that updates all variables efficiently.
- Numerical results show that our solution can effectively improve the system performance and the deployment of RIS can significantly benefit the FD ISAC system.

∗ Corresponding author.
The work of Yang Liu was supported in part by Grant DUT20RC(3)029 and in part by the Open Research Project Programme of the State Key Laboratory of Internet of Things for Smart City (University of Macau) under Grant SKLIoTSC(UM)-2021-2023/ORP/GA01/2022.

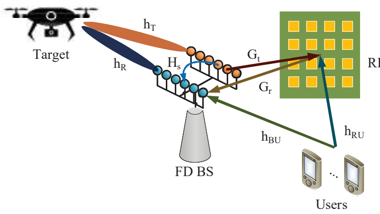

Fig. 1. An RIS-aided FD ISAC system.

II. System Model and Problem Formulation

A. System Model

As shown in Fig. 1, an RIS aided FD ISAC network is considered, where a FD BS equipped N_t transmit (TX) antennas and N_r receive (RX) antennas serves K single-antenna mobile users with the help of an RIS consisting M reflecting units and detects a point-like target simultaneously. For convenience, the sets of users and RIS units are denoted by $\mathcal{K} = \{1, \cdots, K\}$ and $\mathcal{M} = \{1, \cdots, M\}$, respectively. RIS is employed in the vicinity of mobile users.

To conduct target sensing, the BS emits probing signal towards the target from its TX antennas and simultaneously receives the rebounding echoes from the target by its RX antennas. Meanwhile, the FD BS also executes communication functionality by receiving the UL signals transmitted from the mobile users.

Specifically, the probing signal transmitted by the BS can be represented as

$$\mathbf{x} = \mathbf{W}\mathbf{s}_r, \tag{1}$$

where the vector $\mathbf{s}_r \in \mathbb{C}^{N_t \times 1}$ is the probing signal and has zero mean and covariance matrix $\mathbb{E}\{\mathbf{s}_r\mathbf{s}_r^H\} = \mathbf{I}_{N_t}$ and the matrix $\mathbf{W} \in \mathbb{C}^{N_t \times N_t}$ denotes the digital baseband beamformer for the probing signal.

The UL signal of k-th UL user is given as

$$x_{u,k} = \sqrt{q_k} s_{u,k}, \forall k \in \mathcal{K}, \tag{2}$$

where $s_{u,k}$ and q_k are the information symbol and transmission power of k-th user, respectively. For simplicity, we assume that $s_{u,k}$ are circularly symmetric complex Gaussian (CSCG) random variables with zero mean and unit covariance, i.e., $s_k \sim \mathcal{CN}(0, 1)$.

At the same time, the received signals at the BS is expressed as

$$\begin{aligned} \mathbf{y} = &\sum\nolimits_{k=1}^{K} (\mathbf{h}_{BU,k} + \mathbf{G}_r^H \boldsymbol{\Phi} \mathbf{h}_{RU,k}) x_{u,k} \\ &+ \alpha \mathbf{h}_R \mathbf{h}_T^H \mathbf{x} + (\mathbf{G}_r^H \boldsymbol{\Phi} \mathbf{G}_t + \mathbf{H}_s^H)\mathbf{x} + \mathbf{n}_{BS}, \end{aligned} \tag{3}$$

where $\mathbf{G}_t \in \mathbb{C}^{M \times N_t}$, $\mathbf{G}_r \in \mathbb{C}^{M \times N_r}$, $\mathbf{h}_{BU,k} \in \mathbb{C}^{N_r \times 1}$, $\mathbf{h}_{RU,k} \in \mathbb{C}^{M \times 1}$, $\mathbf{h}_T \in \mathbb{C}^{N_t \times 1}$, $\mathbf{h}_R \in \mathbb{C}^{N_r \times 1}$ and $\mathbf{H}_s \in \mathbb{C}^{N_t \times N_r}$ represent the BS-RIS, the RIS-BS, the BS-kth user, the RIS-kth user, the BS-target, the target-BS and the self-interference (SI) channels, respectively. In our setting, we assume that the RIS is employed in the vicinity of mobile users while is far away from the radar target. Besides, signals experienced reflections more than two times are neglected due to significant attenuation. The diagonal matrix $\boldsymbol{\Phi} \triangleq \mathrm{Diag}(\boldsymbol{\phi})$ represents the RIS' reflection coefficients, where the complex vector $\boldsymbol{\phi} = [e^{j\theta_1}, \ldots, e^{j\theta_M}]^T$ is the phase-shifting conducted by the RIS elements to their impinging signals, with θ_m representing the phase shift of m-th reflecting unit, $\theta_m \in [0, 2\pi)$ and $\forall m \in \mathcal{M}$. The coefficient α denotes the target radar cross section (RCS) and $\mathbb{E}\{|\alpha|^2\} = \sigma_t^2$, and the CSCG random vector $\mathbf{n}_{BS} \sim \mathcal{CN}(0, \mathbf{I}_{N_r})$ represents the receiving noise at the BS.

To recover different users' information and improve target sensing performance, the BS utilizes $K+1$ linear filter $\mathbf{u}_j \in \mathbb{C}^{N_r \times 1}$, $\forall j \in \mathcal{J} \triangleq \{0\} \bigcup \mathcal{K}$ to post-process the received signal, where index 0 corresponds to the radar sensing filter bank. Therefore, the output of the j-th post-processor is given as

$$y_j = \mathbf{u}_j^H \mathbf{y}, \ \forall j \in \mathcal{J}. \tag{4}$$

Therefore, the signal-to-interference-and-noise-ratio (SINR) of the output of the radar and mobile users' post-processor are respectively given as

$$\begin{aligned} &\mathrm{SINR}_r(\mathbf{W}, \mathbf{u}_0, \{q_k\}, \boldsymbol{\phi}) = \\ &\frac{\|\mathbf{u}_0^H \mathbf{H} \mathbf{W}\|_2^2}{\sum_{k=1}^{K} q_k |\mathbf{u}_0^H \mathbf{h}_{U,k}|^2 + \|\mathbf{u}_0^H \mathbf{G} \mathbf{W}\|_2^2 + \sigma_r^2 \|\mathbf{u}_0^H\|_2^2}, \end{aligned} \tag{5}$$

$$\begin{aligned} &\mathrm{SINR}_{U,k}(\mathbf{W}, \mathbf{u}_k, \{q_k\}, \boldsymbol{\phi}) = \\ &\frac{q_k |\mathbf{u}_k^H \mathbf{h}_{U,k}|^2}{\sum_{i \neq k}^{K} q_i |\mathbf{u}_k^H \mathbf{h}_{U,i}|^2 + \|\mathbf{u}_k^H \mathbf{H} \mathbf{W}\|_2^2 + \|\mathbf{u}_k^H \mathbf{G} \mathbf{W}\|_2^2 + \sigma_r^2 \|\mathbf{u}_k^H\|_2^2}, \end{aligned} \tag{6}$$

where $\mathbf{H} \triangleq \alpha \mathbf{h}_R \mathbf{h}_T^H$, $\mathbf{G} \triangleq \mathbf{G}_r^H \boldsymbol{\Phi} \mathbf{G}_t + \mathbf{H}_s^H$ and $\mathbf{h}_{U,k} \triangleq \mathbf{h}_{BU,k} + \mathbf{G}_r^H \boldsymbol{\Phi} \mathbf{h}_{RU,k}$.

The UL communication rate of the k-th user is given by

$$\mathrm{R}_k(\mathbf{W}, \mathbf{u}_k, \{q_k\}, \boldsymbol{\phi}) = \log(1 + \mathrm{SINR}_{U,k}), \forall k \in \mathcal{K}. \tag{7}$$

B. Problem Formulation

In this paper, we aim to jointly optimize the transmit beamformer $\mathbf{W}$, the linear post-processing filters $\{\mathbf{u}_k\}_0^K$, the users' UL transmission power $\{q_k\}$ and the reflection phase shift $\boldsymbol{\phi}$ to maximize the sum-rate of all UL mobile users while assuring the target sensing SINR remain above a predefined level. Therefore, the optimization problem is formulated as

$$(\mathrm{P0}): \max_{\mathbf{W}, \mathbf{u}_0, \{\mathbf{u}_k\}, \{q_k\}, \boldsymbol{\phi}} \sum\nolimits_{k=1}^{K} \mathrm{R}_k(\mathbf{W}, \mathbf{u}_k, \{q_k\}, \boldsymbol{\phi}) \tag{8a}$$

$$\text{s.t. } \mathrm{SINR}_r \geq \Gamma_r, \tag{8b}$$

$$\|\mathbf{W}\|_F^2 \leq P_{BS}, \tag{8c}$$

$$q_k \leq P_{U,k}, \forall k \in \mathcal{K}, \tag{8d}$$

$$|\phi_m| = 1, \forall m \in \mathcal{M}, \tag{8e}$$

where Γ_r, P_{BS} and $P_{U,k}$ are denoted as the predefined level of target sensing quality, the transmission power budget of the BS and the transmission power budget of k-th user, respectively. It is obvious that the problem (P0) is highly challenging due to its non-convex objective and constraints.

III. Proposed Algorithm

A. Problem Reformulation

In order to make the problem (P0) more tractable, we firstly employ the weighted mean square error (WMMSE) method [12] to equivalently transform its objective function. Specifically, via introducing auxiliary variables $\{\beta_k\}$ and $\{\omega_k\}$,

$$
\begin{aligned}
&\mathrm{R}_k(\mathbf{W},\mathbf{u}_k,\{q_k\},\boldsymbol{\phi}) \qquad\qquad (9)\\
&=\max_{\omega_k\geq 0}\log(\omega_k)-\omega_k\big(\sum\nolimits_{i=1}^{K}q_i|\mathbf{u}_k^H\mathbf{h}_{U,k}|^2+\|\mathbf{u}_k^H\mathbf{H}\mathbf{W}\|_2^2+\|\mathbf{u}_k^H\mathbf{G}\mathbf{W}\|_2^2+\sigma_r^2\|\mathbf{u}_k^H\|_2^2\big)^{-1}\sqrt{q_k}\mathbf{u}_k^H\mathbf{h}_{U,k}+1\\
&=\max_{\omega_k\geq 0,\beta_k}\underbrace{\log(\omega_k)-\omega_k\bigg(1-2\mathrm{Re}\{\beta_k^*\sqrt{q_k}\mathbf{u}_k^H\mathbf{h}_{U,k}\}+|\beta_k|^2\big(\sum\nolimits_{i=1}^{K}q_i|\mathbf{u}_k^H\mathbf{h}_{U,k}|^2+\|\mathbf{u}_k^H\mathbf{H}\mathbf{W}\|_2^2+\|\mathbf{u}_k^H\mathbf{G}\mathbf{W}\|_2^2+\sigma_r^2\|\mathbf{u}_k^H\|_2^2\big)\bigg)}_{\tilde{\mathrm{R}}_k(\mathbf{W},\mathbf{u}_k,\{q_k\},\boldsymbol{\phi},\omega_k,\beta_k)}+1,\forall k\in\mathcal{K}.
\end{aligned}
$$

the original objective function (8a) can be equivalently written into a variation form [12], as shown in (9) on the top of this page. Therefore, the original problem (P0) can be reformulated as

$$
\begin{aligned}
\text{(P1)}:\ \max_{\substack{\mathbf{W},\mathbf{u}_0,\{\mathbf{u}_k\},\\ \{q_k\},\boldsymbol{\phi},\{\omega_k\},\{\beta_k\}}}\ &\sum\nolimits_{k=1}^{K}\tilde{\mathrm{R}}_k(\mathbf{W},\mathbf{u}_k,\{q_k\},\boldsymbol{\phi},\omega_k,\beta_k) &(10a)\\
\text{s.t. }&\mathrm{SINR}_r\geq\Gamma_r, &(10b)\\
&\|\mathbf{W}\|_F^2\leq P_{BS}, &(10c)\\
&q_k\leq P_{U,k},\forall k\in\mathcal{K}, &(10d)\\
&|\phi_m|=1,\forall m\in\mathcal{M}. &(10e)
\end{aligned}
$$

In the following, we propose to utilize the block descent ascent (BCA) [13] method to tackle the problem (P1).

B. Optimizing Auxiliary Variables $\{\beta_k\}$, $\{\omega_k\}$

According to the derivation of WMMSE transformation, with given other variables, the auxiliary variables $\{\beta_k\}$ and $\{\omega_k\}$ can be updated by the closed form solutions that are given as follows

$$
\beta_k^\star=\frac{\sqrt{q_k}\mathbf{u}_k^H\mathbf{h}_{U,k}}{\sum_{i=1}^{K}q_i|\mathbf{u}_k^H\mathbf{h}_{U,i}|^2+\|\mathbf{u}_k^H\mathbf{H}\mathbf{W}\|_2^2+\|\mathbf{u}_k^H\mathbf{G}\mathbf{W}\|_2^2+\sigma_r^2\|\mathbf{u}_k^H\|_2^2}, \quad (11)
$$

$$
\omega_k^\star=1+\frac{q_k\mathbf{h}_{U,k}^H\mathbf{u}_k\mathbf{u}_k^H\mathbf{h}_{U,k}}{\sum_{i\neq k}^{K}q_i|\mathbf{u}_k^H\mathbf{h}_{U,i}|^2+\|\mathbf{u}_k^H\mathbf{H}\mathbf{W}\|_2^2+\|\mathbf{u}_k^H\mathbf{G}\mathbf{W}\|_2^2+\sigma_r^2\|\mathbf{u}_k^H\|_2^2}. \quad (12)
$$

C. Updating The BS Beamformer $\mathbf{W}$

In this subsection, we will investigate the update of the transmit beamformer $\mathbf{W}$. When other variables are given, the optimization with respect to (w.r.t.) $\mathbf{W}$ is meant to solve

$$
\begin{aligned}
\text{(P2)}:\ \min_{\mathbf{w}}\ &\mathbf{w}^H\mathbf{D}_1\mathbf{w}-c_1 &(13a)\\
\text{s.t. }&\mathbf{w}^H\mathbf{D}_2\mathbf{w}-\mathbf{w}^H\mathbf{D}_3\mathbf{w}+c_2\leq 0, &(13b)\\
&\mathbf{w}^H\mathbf{w}\leq P_{BS}. &(13c)
\end{aligned}
$$

with the new parameters above defined as follows

$$
\begin{aligned}
&\mathbf{w}\triangleq\mathrm{vec}(\mathbf{W}), c_2\triangleq(\sum\nolimits_{k=1}^{K}q_k|\mathbf{u}_0^H\mathbf{h}_{U,k}|^2+\sigma_r^2\|\mathbf{u}_0^H\|_2^2), \qquad (14)\\
&\mathbf{D}_2\triangleq\mathbf{I}_{N_t}\otimes\mathbf{G}^H\mathbf{u}_0\mathbf{u}_0^H\mathbf{G}, \mathbf{D}_3\triangleq(\mathbf{I}_{N_t}\otimes\mathbf{H}^H\mathbf{u}_0\mathbf{u}_0^H\mathbf{H})/\Gamma_r,\\
&c_1=\big[\sum\nolimits_{k=1}^{K}\big(\log(\omega_k)-\omega_k+2\mathrm{Re}\{\omega_k\beta_k^*\sqrt{q_k}\mathbf{u}_k^H\mathbf{h}_{U,k}\}\\
&\quad-\omega_k|\beta_k|^2(\sum\nolimits_{i=1}^{K}q_i|\mathbf{u}_k^H\mathbf{h}_{U,i}|^2+\sigma_r^2\|\mathbf{u}_k^H\|_2^2)+1\big)\big],\\
&\mathbf{D}_1\triangleq\sum\nolimits_{k=1}^{K}\omega_k|\beta_k|^2(\mathbf{I}_{N_t}\otimes\mathbf{H}^H\mathbf{u}_k\mathbf{u}_k^H\mathbf{H}+\mathbf{I}_{N_t}\otimes\mathbf{G}^H\mathbf{u}_k\mathbf{u}_k^H\mathbf{G}).
\end{aligned}
$$

Note that the problem (P2) is difficult due to the difference of convex (DC) form constraint (13b). Therefore, we linearize the concave quadratic term $\mathbf{w}^H\mathbf{D}_3\mathbf{w}$ in (13b) at a point $\mathbf{w}_0$ via the MM framework [10] as follows

$$
\mathbf{w}^H\mathbf{D}_3\mathbf{w}\geq 2\mathrm{Re}\{\mathbf{w}_0^H\mathbf{D}_3(\mathbf{w}-\mathbf{w}_0)\}+\mathbf{w}_0^H\mathbf{D}_3\mathbf{w}_0, \quad (15)
$$

where $\mathbf{w}_0$ is the value of $\mathbf{w}$ obtained in the last iteration. Next, we replace the constraint (13b) by (15) and the optimization problem (P2) is rewritten as

$$
\begin{aligned}
\text{(P3)}:\ \min_{\mathbf{w}}\ &\mathbf{w}^H\mathbf{D}_1\mathbf{w}-c_1 &(16a)\\
\text{s.t. }&\mathbf{w}^H\mathbf{D}_2\mathbf{w}-2\mathrm{Re}\{\mathbf{d}_3^H\mathbf{w}\}+\hat{c}_2\leq 0, &(16b)\\
&\mathbf{w}^H\mathbf{w}\leq P_{BS}, &(16c)
\end{aligned}
$$

where $\mathbf{d}_3\triangleq\mathbf{D}_3^H\mathbf{w}_0$ and $\hat{c}_2\triangleq c_2+(\mathbf{w}_0^H\mathbf{D}_3\mathbf{w}_0)^*$. The problem (P3) is a typical second order cone program (SOCP) and can be solved by off-the-shelf numerical solvers, e.g., CVX [14].

D. Optimizing The User Transmission Power

With other variables being fixed, the optimization of all the users' transmission power $\{q_k\}$ is reduced to solve

$$
\begin{aligned}
\text{(P4)}:\ \min_{\{q_k\}}\ &\sum\nolimits_{k=1}^{K}a_kq_k+\sum\nolimits_{k=1}^{K}b_k\sqrt{q_k}-c_3 &(17a)\\
\text{s.t. }&\sum\nolimits_{k=1}^{K}d_kq_k\leq\hat{c}_3, &(17b)\\
&0\leq q_k\leq P_{U,k},\forall k\in\mathcal{K}, &(17c)
\end{aligned}
$$

where the newly introduced coefficients are defined as follows

$$
\begin{aligned}
&a_k\triangleq\sum\nolimits_{j=1}^{K}\omega_j|\beta_j|^2|\mathbf{u}_j^H\mathbf{h}_{U,k}|^2, d_k\triangleq|\mathbf{u}_0^H\mathbf{h}_{U,k}|^2, \qquad (18)\\
&\hat{c}_3\triangleq\|\mathbf{u}_0^H\mathbf{H}\mathbf{W}\|_2^2/\Gamma_r-\|\mathbf{u}_0^H\mathbf{G}\mathbf{W}\|_2^2-\sigma_r^2\|\mathbf{u}_0^H\|_2^2,\\
&b_k\triangleq-2\mathrm{Re}(\omega_k\beta_k^*\mathbf{u}_k^H\mathbf{h}_{U,k}), c_3\triangleq\sum\nolimits_{k=1}^{K}\big\{\log(\omega_k)-\omega_k\\
&\quad-\omega_k|\beta_k|^2(\|\mathbf{u}_k^H\mathbf{H}\mathbf{W}\|_2^2+\|\mathbf{u}_k^H\mathbf{G}\mathbf{W}\|_2^2+\sigma_r^2\|\mathbf{u}_k^H\|)+1\big\}.
\end{aligned}
$$

The problem (P4) can still be formulated into an SOCP problem and can be numerically solved.

E. Optimizing The Users' Filters $\{\mathbf{u}_k\}_{k=1}^K$

The update of $\{\mathbf{u}_k\}$ are meant to solve the following problem

$$
\text{(P5)}:\ \min_{\{\mathbf{u}_k\}}\ \sum\nolimits_{k=1}^{K}(\mathbf{u}_k^H\mathbf{F}_k\mathbf{u}_k-2\mathrm{Re}\{\mathbf{u}_k^H\tilde{\mathbf{h}}_{U,k}\})-c_4 \quad (19)
$$

where the parameters of (P5) are defined as

$$
\begin{aligned}
&\tilde{\mathbf{h}}_{U,k}\triangleq\omega_k\beta_k^*\sqrt{q_k}\mathbf{h}_{U,k}, c_4\triangleq\sum\nolimits_{k=1}^{K}\big(\log(\omega_k)+\omega_k+1\big), \qquad (20)\\
&\mathbf{F}_k\triangleq\omega_k|\beta_k|^2\big(\sum\nolimits_{i=1}^{K}q_i\mathbf{h}_{U,i}\mathbf{h}_{U,i}^H+\mathbf{H}\mathbf{W}\mathbf{W}^H\mathbf{H}^H+\mathbf{G}\mathbf{W}\mathbf{W}^H\mathbf{G}^H+\sigma_r^2\mathbf{I}_{N_r}\big).
\end{aligned}
$$

Hence the problem (P5) can be decomposed into K independent sub-problems with each being given as

$$
(\mathrm{P6_k}):\ \min_{\mathbf{u}_k}\ \mathbf{u}_k^H\mathbf{F}_k\mathbf{u}_k-2\mathrm{Re}\{\mathbf{u}_k^H\tilde{\mathbf{h}}_{U,k}\} \quad (21)
$$

Notice that the problem ($\mathrm{P6_k}$) is a typical unconstrained convex quadratic problem. Its optimal solution can be easily obtained via setting its derivative as zero and obtained as follows

$$\mathbf{u}_k^\star = \mathbf{F}_k^{-1}\tilde{\mathbf{h}}_{U,k}, \forall k \in \mathcal{K}. \tag{22}$$

F. Optimizing Radar Filter $\mathbf{u}_0$

When other variables are given, the optimization problem w.r.t. $\mathbf{u}_0$ is reduced to a feasibility characterization problem, which is given as

$$\text{(P7)}: \text{Find } \mathbf{u}_0 \tag{23a}$$

$$\text{s.t. } \mathbf{u}_0^H\mathbf{E}_1\mathbf{u}_0 - \mathbf{u}_0^H\mathbf{E}_2\mathbf{u}_0 \le 0. \tag{23b}$$

where the parameters of problem (P7) are defined as

$$\mathbf{E}_2 \triangleq \mathbf{H}\mathbf{W}\mathbf{W}^H\mathbf{H}^H/\Gamma_r, \tag{24}$$

$$\mathbf{E}_1 \triangleq \big(\sum\nolimits_{k=1}^{K} q_k\mathbf{h}_{U,k}\mathbf{h}_{U,k}^H + \mathbf{G}\mathbf{W}\mathbf{W}^H\mathbf{G}^H + \sigma_r^2\mathbf{I}_{N_r}\big).$$

To tackle (P7), we consider another closely related problem as follows

$$\text{(P8)}: \min_{\mathbf{u}_0,\alpha_u} \ \alpha_u \tag{25a}$$

$$\text{s.t. } \mathbf{u}_0^H\mathbf{E}_1\mathbf{u}_0 - \mathbf{u}_0^H\mathbf{E}_2\mathbf{u}_0 \le \alpha_u. \tag{25b}$$

Suppose that the optimal solution ($\mathbf{u}_0^\star$,$\alpha_u^\star$) of (P8) yields $\alpha_u^\star \le 0$, then $\mathbf{u}_0^\star$ is actually a feasible solution to (P7). Therefore, we turn to solve (P8). Note that (P8) is assured to have a solution yielding non-positive objective as long as we start iteration from a feasible solution. It is obvious that the operation of minimizing the variable α_u is equivalent to minimize the left side of the constraint (25b) w.r.t. variable $\mathbf{u}_0$. Therefore, we turn to optimize $\mathbf{u}_0$ and solve the following problem

$$\text{(P9)}: \min_{\mathbf{u}_0} \ \mathbf{u}_0^H\mathbf{E}_1\mathbf{u}_0 - \mathbf{u}_0^H\mathbf{E}_2\mathbf{u}_0 \tag{26}$$

Since the objective function (26) is non-convex due to its DC form, we adopt the MM method to construct a linear low-bound of $\mathbf{u}_0^H\mathbf{E}_2\mathbf{u}_0$, which is given as

$$\begin{aligned}\mathbf{u}_0^H\mathbf{E}_2\mathbf{u}_0 &\ge \hat{\mathbf{u}}_0^H\mathbf{E}_2\hat{\mathbf{u}}_0 + 2\text{Re}\{\hat{\mathbf{u}}_0^H\mathbf{E}_2(\mathbf{u}_0 - \hat{\mathbf{u}}_0)\}\\ &= 2\text{Re}\{\hat{\mathbf{u}}_0^H\mathbf{E}_2\mathbf{u}_0\} - (\hat{\mathbf{u}}_0^H\mathbf{E}_2\hat{\mathbf{u}}_0)^*,\end{aligned} \tag{27}$$

where $\hat{\mathbf{u}}_0$ is feasible solution obtained in the last iteration.

Then replacing the term $\mathbf{u}_0^H\mathbf{E}_2\mathbf{u}_0$ by (27), we turn to optimize a tight convex upper bound of the objective (P9), which is given as

$$\text{(P10)}: \min_{\mathbf{u}_0} \ \mathbf{u}_0^H\mathbf{E}_1\mathbf{u}_0 - 2\text{Re}\{\hat{\mathbf{u}}_0^H\mathbf{E}_2\mathbf{u}_0\} + (\hat{\mathbf{u}}_0^H\mathbf{E}_2\hat{\mathbf{u}}_0)^* \tag{28}$$

The problem (P10) is a unconstraint convex quadratic problem and its optimal solution is directly given as

$$\mathbf{u}_0^\star = \mathbf{E}_1^{-1}(\mathbf{E}_2^H\hat{\mathbf{u}}_0). \tag{29}$$

G. Optimizing The Phase Shift $\boldsymbol{\phi}$

In this subsection, we investigate the optimization of the phase shift $\boldsymbol{\phi}$. By introducing the new definitions as follows

$$\begin{aligned}&\mathbf{P}_k \triangleq \mathbf{G}_r^H\text{diag}(\mathbf{h}_{RU,k}), \mathbf{r}_k \triangleq \mathbf{G}_r\mathbf{u}_k,\\ &\mathbf{S}_k \triangleq \mathbf{W}^H\mathbf{G}_t^H\text{diag}(\mathbf{r}_k), \mathbf{v}_k \triangleq \mathbf{u}_k^H\mathbf{H}_s^H\mathbf{W},\\ &\mathbf{r}_0 \triangleq \mathbf{G}_r\mathbf{u}_0, \mathbf{S}_0 \triangleq \mathbf{W}^H\mathbf{G}_t^H\text{diag}(\mathbf{r}_0), \mathbf{v}_0 \triangleq \mathbf{u}_0^H\mathbf{H}_s^H\mathbf{W},\end{aligned} \tag{30}$$

the objective function (10a) and the constraint (10b) can be respectively rewritten as

$$-\sum\nolimits_{k=1}^{K}\tilde{\text{R}}_k = \boldsymbol{\phi}^H\mathbf{T}\boldsymbol{\phi} - 2\text{Re}\{\mathbf{x}^H\boldsymbol{\phi}\} - c_5, \tag{31a}$$

$$\boldsymbol{\phi}^H\mathbf{T}_0\boldsymbol{\phi} - 2\text{Re}\{\mathbf{x}_0^H\boldsymbol{\phi}\} + c_6 \le 0, \tag{31b}$$

with the parameters in (31a) and (31b) being defined in (32), as shown on the top of next page.

Based on the above transformation, the optimization problem w.r.t. $\boldsymbol{\phi}$ is reduced to

$$\text{(P11)}: \min_{\boldsymbol{\phi}} \ \boldsymbol{\phi}^H\mathbf{T}\boldsymbol{\phi} - 2\text{Re}\{\mathbf{x}^H\boldsymbol{\phi}\} - c_5 \tag{33a}$$

$$\text{s.t. } \boldsymbol{\phi}^H\mathbf{T}_0\boldsymbol{\phi} - 2\text{Re}\{\mathbf{x}_0^H\boldsymbol{\phi}\} + c_6 \le 0, \tag{33b}$$

$$|\phi_m| = 1, \forall m \in \mathcal{M}. \tag{33c}$$

Due to the nonlinear equality constraint (33c), the problem (P11) is non-convex. To resolve (P11), we adopt the PDD method [11]. Firstly, to decouple the nonconvex constraints (33c), we introduce an auxiliary variable $\boldsymbol{\psi}$ and transform problem (P11) as follows

$$\text{(P12)}: \min_{\boldsymbol{\phi},\boldsymbol{\psi}} \ \boldsymbol{\phi}^H\mathbf{T}\boldsymbol{\phi} - 2\text{Re}\{\mathbf{x}^H\boldsymbol{\phi}\} - c_5 \tag{34a}$$

$$\text{s.t. } \boldsymbol{\phi}^H\mathbf{T}_0\boldsymbol{\phi} - 2\text{Re}\{\mathbf{x}_0^H\boldsymbol{\phi}\} + c_6 \le 0, \tag{34b}$$

$$\boldsymbol{\phi} = \boldsymbol{\psi}, \tag{34c}$$

$$|\psi_m| = 1, \forall m \in \mathcal{M}. \tag{34d}$$

Next, via penalizing the equality constraint (34c), the augmented Lagrangian (AL) problem of (P12) is given as

$$\begin{aligned}\text{(P13)}: \min_{\boldsymbol{\phi},\boldsymbol{\psi},\rho,\boldsymbol{\lambda}} \ &\boldsymbol{\phi}^H\mathbf{T}\boldsymbol{\phi} - 2\text{Re}\{\mathbf{x}^H\boldsymbol{\phi}\} - c_5\\ &+ \frac{1}{2\rho}\|\boldsymbol{\phi} - \boldsymbol{\psi}\|_2^2 + \text{Re}\{\boldsymbol{\lambda}^H(\boldsymbol{\phi} - \boldsymbol{\psi})\}\end{aligned} \tag{35a}$$

$$\text{s.t. } \boldsymbol{\phi}^H\mathbf{T}_0\boldsymbol{\phi} - 2\text{Re}\{\mathbf{x}_0^H\boldsymbol{\phi}\} + c_6 \le 0, \tag{35b}$$

$$|\psi_m| = 1, \forall m \in \mathcal{M}. \tag{35c}$$

where ρ is the penalty coefficient and $\boldsymbol{\lambda}$ is the Lagrangian multiplier associated with (34c). Guided by the PDD framework [11], we conduct a two-layer iteration procedure, with its inner layer alternatively updating $\boldsymbol{\phi}$ and $\boldsymbol{\psi}$ in a block coordinate descent (BCD) manner while the outer layer selectively updating the penalty coefficient ρ or the dual variable $\boldsymbol{\lambda}$. The PDD procedure will be elaborated in the following.

Inner Layer Procedure

For the inner layer iteration, we alternatively update $\boldsymbol{\phi}$ and $\boldsymbol{\psi}$. When $\boldsymbol{\psi}$ is given, the minimization of AL w.r.t. $\boldsymbol{\phi}$ reduces to solving the following problem

$$\begin{aligned}\text{(P14)}: \min_{\boldsymbol{\phi}} \ &\boldsymbol{\phi}^H\mathbf{T}\boldsymbol{\phi} - 2\text{Re}\{\mathbf{x}^H\boldsymbol{\phi}\} - c_5\\ &+ \frac{1}{2\rho}\|\boldsymbol{\phi} - \boldsymbol{\psi}\|_2^2 + \text{Re}\{\boldsymbol{\lambda}^H(\boldsymbol{\phi} - \boldsymbol{\psi})\}\end{aligned} \tag{36a}$$

$$\text{s.t. } \boldsymbol{\phi}^H\mathbf{T}_0\boldsymbol{\phi} - 2\text{Re}\{\mathbf{x}_0^H\boldsymbol{\phi}\} + c_6 \le 0. \tag{36b}$$

The problem (P14) is an SOCP and can be solved by CVX.

When $\boldsymbol{\phi}$ is fixed, the update of the auxiliary variable $\boldsymbol{\psi}$ is meant to solve

$$\text{(P15)}: \min_{\boldsymbol{\psi}} \ \frac{1}{2\rho}\|\boldsymbol{\phi} - \boldsymbol{\psi}\|_2^2 + \text{Re}\{\boldsymbol{\lambda}^H(\boldsymbol{\phi} - \boldsymbol{\psi})\} \tag{37a}$$

$$\text{s.t. } |\psi_m| = 1, \forall m \in \mathcal{M}. \tag{37b}$$

It is readily seen that the quadratic term w.r.t. $\boldsymbol{\psi}$ in the objective function (37a) is constant, i.e., $\|\boldsymbol{\psi}\|_2^2/(2\rho) = M/(2\rho)$ since $\boldsymbol{\psi}$ has unit modulus entries. Therefore, the problem (P15) is equivalently written as

$$\text{(P16)}: \max_{|\boldsymbol{\psi}|=\mathbf{1}_M} \ \text{Re}\{(\boldsymbol{\phi} + \rho\boldsymbol{\lambda})^H\boldsymbol{\psi}\} \tag{38}$$

Note that the maximum of problem (P16) can be achieved when the phases of the entries of $\boldsymbol{\psi}$ are all aligned with those of the linear coefficient $(\rho^{-1}\boldsymbol{\phi} + \boldsymbol{\lambda})$, that the optimal solution is given as

$$\boldsymbol{\psi}^\star = \exp\big(j \cdot \angle(\boldsymbol{\phi} + \rho\boldsymbol{\lambda})\big). \tag{39}$$

The objective value of (P13) will achieve monotonically converge by alternatively updating $\boldsymbol{\phi}$ and $\boldsymbol{\psi}$ via BCD method in the inner layer.

$$
\begin{aligned}
&c_6 \triangleq \left(\sum_{k=1}^{K} q_k \mathbf{u}_0^H \mathbf{h}_{BU,k}\mathbf{h}_{BU,k}^H \mathbf{u}_0 + \mathbf{v}_0\mathbf{v}_0^H + \sigma_r^2\|\mathbf{u}_0^H\|_2^2\right) - \|\mathbf{u}_0^H\mathbf{H}\mathbf{W}\|_2^2/\Gamma_r, \\
&\mathbf{T} \triangleq \sum_{k=1}^{K}\left\{\omega_k|\beta_k|^2\left[\sum_{i=1}^{K} q_i(\mathbf{P}_i^H\mathbf{u}_k\mathbf{u}_k^H\mathbf{P}_i) + \mathbf{S}_k^T\mathbf{S}_k^*\right]\right\}, \mathbf{T}_0 \triangleq \left(\sum_{k=1}^{K} q_k\mathbf{P}_k^H\mathbf{u}_0\mathbf{u}_0k^H\mathbf{P}_k + \mathbf{S}_0^T\mathbf{S}_0^*\right), \\
&\mathbf{x}_0 \triangleq -\left(\sum_{k=1}^{K} q_k(\mathbf{h}_{BU,k}^H\mathbf{u}_0\mathbf{u}_0^H\mathbf{P}_k) + \mathbf{v}_0^*\mathbf{S}_0^*\right)^H, \mathbf{x} \triangleq \sum_{k=1}^{K}\left\{\omega_k\beta_k^*\sqrt{q_k}\mathbf{u}_k^H\mathbf{P}_k - \omega_k|\beta_k|^2\left[\sum_{i=1}^{K} q_i(\mathbf{h}_{BU,i}^H\mathbf{u}_k\mathbf{u}_k^H\mathbf{P}_i) + \mathbf{v}_k^*\mathbf{S}_k^*\right]\right\}^H, \\
&c_5 \triangleq \sum_{k=1}^{K}\{\log(\omega_k) - \omega_k + 1 + 2\mathrm{Re}\{\omega_k\beta_k^*\sqrt{q_k}\mathbf{u}_k^H\mathbf{h}_{BU,k}\} - \omega_k|\beta_k|^2[\sum_{i=1}^{K} q_i\mathbf{u}_k^H\mathbf{h}_{BU,i}\mathbf{h}_{BU,i}^H\mathbf{u}_k + \|\mathbf{u}_k^H\mathbf{H}\mathbf{W}\|_2^2 + \mathbf{v}_k\mathbf{v}_k^H + \sigma_r^2\|\mathbf{u}_k^H\|_2^2]\}.
\end{aligned} \tag{32}
$$

Algorithm 1 PDD Method to Solve (P11)

initialize $\boldsymbol{\phi}^{(0)}$, $\boldsymbol{\psi}^{(0)}$, $\boldsymbol{\lambda}^{(0)}$, $\rho^{(0)}$ and $k = 1$;
repeat
  set $\boldsymbol{\phi}^{(k-1,0)} := \boldsymbol{\phi}^{(k-1)}$, $\boldsymbol{\psi}^{(k-1,0)} := \boldsymbol{\psi}^{(k-1)}$, $t = 0$;
  repeat
    update $\boldsymbol{\phi}^{(k-1,t+1)}$ by solving (P14);
    update $\boldsymbol{\psi}^{(k-1,t+1)}$ by (39);
    $t++$;
  until *convergence*
  set $\boldsymbol{\phi}^{(k)} := \boldsymbol{\phi}^{(k-1,\infty)}$, $\boldsymbol{\psi}^{(k)} := \boldsymbol{\psi}^{(k-1,\infty)}$;
  if $\|\boldsymbol{\phi}^{(k)} - \boldsymbol{\psi}^{(k)}\|_\infty \leq \eta_k$ **then**
    $\boldsymbol{\lambda}^{(k+1)} := \boldsymbol{\lambda}^{(k)} + \frac{1}{\rho^{(k)}}(\boldsymbol{\phi}^{(k)} - \boldsymbol{\psi}^{(k)})$, $\rho^{(k+1)} := \rho^{(k)}$;
  else
    $\boldsymbol{\lambda}^{(k+1)} := \boldsymbol{\lambda}^{(k)}$, $1/\rho^{(k+1)} := 1/(c \cdot \rho^{(k)})$;
  end if
  $k++$;
until $\|\boldsymbol{\phi}^{(k)} - \boldsymbol{\psi}^{(k)}\|_2$ is sufficiently small;

Outer Layer Procedure

In the outer layer, we adjust the value of dual variable $\boldsymbol{\lambda}$ or the penalty coefficient ρ. Specifically,

1) when $\boldsymbol{\phi} = \boldsymbol{\psi}$ is approximately achieved, i.e., $\|\boldsymbol{\psi} - \boldsymbol{\phi}\|_\infty$ is smaller than some predefined diminishing threshold η_k [11], the dual variable $\boldsymbol{\lambda}$ will be updated in a gradient ascent manner as follows:
$$\boldsymbol{\lambda}^{(k+1)} := \boldsymbol{\lambda}^{(k)} + \rho^{-1}(\boldsymbol{\phi} - \boldsymbol{\psi}); \tag{40}$$
2) if the equality constraint $\boldsymbol{\phi} = \boldsymbol{\psi}$ is far from "being true", for achieving $\boldsymbol{\phi} = \boldsymbol{\psi}$ in the subsequent iterations, the outer layer will increase the penalty parameter ρ^{-1} as follows:
$$\left(\rho^{(k+1)}\right)^{-1} := c^{-1} \cdot \left(\rho^{(k)}\right)^{-1}, \tag{41}$$
where c is a positive constant, whose value is smaller than 1 and typically chosen in the range of [0.8, 0.9].

The PDD-based method to solve problem (P11) is summarized in Algorithm 1. The overall algorithm to solve problem (P1) is specified in Algorithm 2.

Algorithm 2 Proposed Algorithm to Solve (P1)

randomly generate feasible $\boldsymbol{\phi}^{(0)}$, $\mathbf{W}^{(0)}$, $\{q_k^0\}$, $\{\mathbf{u}_k\}$, $\mathbf{u}_0$, and $i = 0$;
repeat
  update $\{\beta_k^{(i+1)}\}$ and $\{\omega_k^{(i+1)}\}$ by (11) and (12), respectively.
  set $\mathbf{W}^{(i,0)} := \mathbf{W}^{(i)}$, $m = 0$;
  repeat
    update $\mathbf{W}^{(i,m+1)}$ by solving (P3);
    $m++$;
  until *convergence*;
  set $\mathbf{W}^{(i+1)} := \mathbf{W}^{(i,\infty)}$;
  update $\{q_k^{(i+1)}\}$ by solving (P4);
  update $\{\mathbf{u}_k^{(i+1)}\}$ by (22);
  set $\mathbf{u}_0^{(i,0)} := \mathbf{u}_0^{(i)}$, $m = 0$;
  repeat
    update $\mathbf{u}_0^{(i,m+1)}$ by (29);
    $m++$;
  until *convergence*;
  set $\mathbf{u}_0^{(i+1)} := \mathbf{u}_0^{(i,\infty)}$;
  update $\boldsymbol{\phi}^{(i+1)}$ by invoking Alg.1;
  $i++$;
until *convergence*;

IV. Numerical Results

In this section, we will provide numerical results to verify the performance of our proposed algorithm. The setting of the experiment is shown in Fig. 2, where one FD BS serves 4 users aided by an RIS and attempts to detect 1 point target simultaneously. In the experiment, We assume that the locations of BS, RIS and target are (0,0,4.5m), (0,−100m,2.5m) and (0,6m,12.5m), respectively. Besides, all users are randomly distributed within a right half circle of the radius of 10m centered at the RIS at an altitude of 1.5m. The SI and BS-RIS links are assumed to be Rician fading channel model with Rician factor of 5dB and 4dB, respectively. The BS-User links and RIS-User links all are assumed to be Rayleigh fading channels. The BS-Target/Target-BS links are modeled as line-of-sight (LoS) channels. The path loss exponents of BS-User, BS-RIS, RIS-User, BS-Target and Target-BS are $\alpha_{BU} = 3.6$, $\alpha_{BR} = 2.7$, $\alpha_{RU} = 2.4$ and $\alpha_{BT} = \alpha_{TB} = 2.2$, respectively. The path loss of SI channel is set to $\rho_{SI} = -110$dB due to the SI cancellation [15]. In addition, we assume that the RIS consists of $M = 100$ units and the BS equips $N_t = N_r = 4$ transmit and receive antennas, respectively. Other parameters setting are $\mathrm{P}_{BS} = 30$dBm, $\sigma_{BS}^2 = -90$dBm, $\Gamma_r = 5$dB and $\sigma_t^2 = 1$.

Fig. 3 illustrates the converge behaviours of our proposed PDD-based method for updating phase shift $\boldsymbol{\phi}$. In Fig. 3, under various settings of RIS units M, the left and right subfigure show the difference between $\boldsymbol{\phi}$ and $\boldsymbol{\psi}$ and the variation in $\boldsymbol{\phi}$ itself along with iteration progress in log domain. As reflected by Fig. 3, with the execution of the PDD method, the variation in $\boldsymbol{\phi}$ and difference between $\boldsymbol{\phi}$ and $\boldsymbol{\psi}$ become

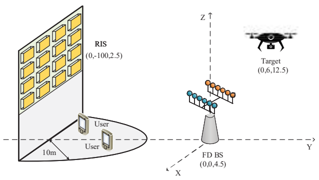

Fig. 2. The experiment setting.

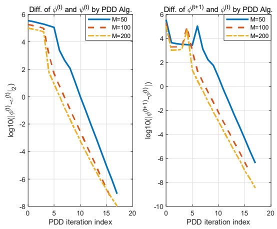

Fig. 3. Convergence of PDD method.

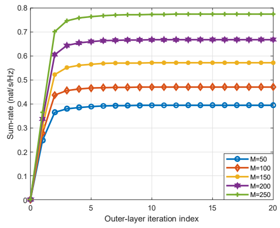

Fig. 4. Convergence of Alg. 2.

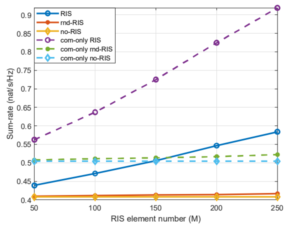

Fig. 5. The impact of M

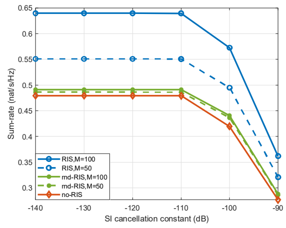

Fig. 6. The impact of SI channel.

negligible (below 10^{-6}) within 20 iterations.

Fig. 4 demonstrates the convergence behaviours of our proposed algorithm with different numbers of RIS' elements. For each specific M, the algorithm generally converges within 10 iterations and yield monotonic improvement in sun-rate.

In Fig. 5, we present the sum-rate versus the number of RIS units. For comparison, we consider the communication-only ("com-only") system. It is clearly shown that increasing the number of RIS elements can boost the sum-rate performance. Moreover, our proposed algorithm ("RIS") significantly outperforms both no RIS ("no-RIS") and random phase-shift RIS ("rnd-RIS") schemes in ISAC and communication-only systems, respectively. Besides, due to the trade-off between the communication and radar sensing performance, we can observe the performance gap between ISAC and communication-only system.

In Fig. 6, we examine the impact of the magnitude of SI channel. The horizontal axis shows the SI coefficient ρ_{SI}, which is proportional to the magnitude of SI channel $\mathbf{H}_S$. As can be seen, sum-rate drops when SI increases. Compared to the no-RIS scenario, the deployment of RIS significantly boosts the sum-rate.

V. Conclusions

In this paper, we investigate the joint active and passive beamforming design problem in an RIS aided FD ISAC system that performs target sensing and UL communication functionality simultaneously. Via utilizing MM and PDD methods, we develop an iterative solution that efficiently updates all variables via convex optimization techniques. Numerical results demonstrate the effectiveness of our proposed algorithm and the benefit of deploying RIS in the FD ISAC system.

References

[1] F. Liu, C. Masouros, A. P. Petropulu, H. Griffiths, and L. Hanzo, "Joint radar and communication design: Applications, state-of-the-art, and the road ahead," *IEEE Trans. Commun.*, vol. 68, no. 6, pp. 3834-3862, Jun. 2020.

[2] F. Liu *et al.*, "Integrated sensing and communications: Toward dual-functional wireless networks for 6G and beyond," *IEEE J. Sel. Areas Commun.*, vol. 40, no. 6, pp. 1728-1767, Jun. 2022.

[3] C. Pan *et al.*, "An overview of signal processing techniques for RIS/IRS-aided wireless systems," *IEEE J. Sel. Topics Signal Process.*, vol. 16, no. 5, pp. 883-917, Aug. 2022.

[4] Q. Wu, S. Zhang, B. Zheng, C. You, and R. Zhang, "Intelligent reflecting surface-aided wireless communications: A tutorial," *IEEE Trans. Commun.* vol. 69, no. 5, pp. 3313-3351, May 2021.

[5] X. Wang, Z. Fei, J. Huang, and H. Yu, "Joint waveform and discrete phase shift design for RIS-assisted integrated sensing and communication system under Cramér-Rao bound constraint," *IEEE Trans. Veh. Technol.*, vol. 71, no. 1, pp. 1004-1009, Jan. 2022.

[6] X. Wang, Z. Fei, Z. Zheng, and J. Guo, "Joint waveform design and passive beamforming for RIS-assisted dual-functional radar-communication system," *IEEE Trans. Veh. Technol.*, vol. 70, no. 5, pp. 5131-5136, May 2021.

[7] Z. -M. Jiang *et al.*, "Intelligent reflecting surface aided dual-function radar and communication system," *IEEE Syst. J.*, vol. 16, no. 1, pp. 475-486, Mar. 2022.

[8] Y. Li and A. Petropulu, "Dual-function radar-communication system aided by intelligent reflecting surfaces," in *Proc. 2022 IEEE 12th Sens. Array Multichannel Signal Process. Workshop (SAM)*, 2022, pp. 126-130.

[9] M. Hua, Q. Wu, C. He, S. Ma, and W. Chen, "Joint active and passive beamforming design for IRS-Aided radar-communication," *IEEE Trans. Wireless Commun.*, early access, October 06, 2022, doi: 10.1109/TWC.2022.3210532.

[10] Y. Sun, P. Babu, and D. P. Palomar, "Majorization-minimization algorithms in signal processing, communications, and machine learning," *IEEE Trans. Signal Process.*, vol. 65, no. 3, pp. 794-816, Feb. 2017.

[11] Q. Shi and M. Hong, "Penalty dual decomposition method for nonsmooth nonconvex optimization-part i : Algorithms and convergence analysis," *IEEE Trans. Signal Process.*, vol. 68, pp. 4108-4122, Jun. 2020.

[12] Q. Shi, M. Razaviyayn, Z. -Q. Luo, and C. He, "An iteratively weighted MMSE approach to distributed sum-utility maximization for a MIMO interfering broadcast channel," *IEEE Trans. Signal Process.*, vol. 59, no. 9, pp. 4331-4340, Sept. 2011.

[13] D. Bertsekas, "Nonlinear programming," 2nd ed. Belmont, MA: Athena Scientific, 1999.

[14] M. Grant and S. Boyd, *CVX: Matlab software for disciplined convex programming*, version 2.1, http://cvxr.com/cvx, Mar. 2014.

[15] Y. Sun, D. W. K. Ng, Z. Ding, and R. Schober, "Optimal joint power and subcarrier allocation for full-duplex multicarrier non-orthogonal multiple access systems," *IEEE Trans. Commun.*, vol. 65, no. 3, pp. 1077-1091, Mar. 2017.